Neuron, Vol. 21, 827–835, October, 1998, Copyright ©1998 by Cell Press

Polarity of Long-Term Synaptic Gain Change Is Related to Postsynaptic Spike Firing at a Cerebellar Inhibitory Synapse

Carlos D. Aizenman,* Paul B. Manis,*† and David J. Linden*‡

*Department of Neuroscience

†Department of Otolaryngology

Head and Neck Surgery

Johns Hopkins University School of Medicine

Baltimore, Maryland 21205

Summary

Long-term potentiation and depression (LTP and LTD) in excitatory synapses can coexist, the former being triggered by stimuli that produce strong postsynaptic excitation and the latter by stimuli that produce weaker postsynaptic excitation. It has not been determined whether these properties also apply to LTP and LTD in the inhibitory synapses between Purkinje neurons and the neurons of the deep cerebellar nuclei (DCN), a site that has been implicated in certain types of motor learning. DCN cells exhibit a prominent rebound depolarization (RD) and associated spike burst upon release from hyperpolarization. In these cells, LTP can be elicited by short, high-frequency trains of inhibitory postsynaptic potentials (IPSPs), which reliably evoke an RD. LTD is induced if the same protocol is applied with conditions where the amount of postsynaptic excitation is reduced. The polarity of the change in synaptic strength is correlated with the amount of RD-evoked spike firing during the induction protocol. Thus, some important computational principles that govern the induction of use-dependent change in excitatory synaptic efficacy also apply to inhibitory synapses.

Introduction

A central hypothesis of contemporary neurobiology is that memory is stored in the brain through use-dependent modifications in the properties of synaptic transmission. The vast majority of work in support of this hypothesis has focused upon two cellular processes, homosynaptic long-term potentiation and depression (LTP and LTD) of excitatory, glutamatergic synaptic transmission. LTP and LTD are typically evoked by brief, high-frequency and sustained, low-frequency stimulation, respectively (Linden and Connor, 1995). These phenomena have been shown to coexist in the same set of synapses and to reverse each other, thus endowing these synapses with use-dependent bidirectional modification, a computationally important feature. A cellular model has emerged to explain the induction phase of LTP and LTD (Bear and Malenka, 1994; Lisman, 1994). In their most frequently studied forms, induction of LTP and LTD are dependent upon the influx of postsynaptic Ca^{2+} through NMDA receptor–associated ion channels and/or voltage-gated Ca^{2+} channels. The direction of change in synaptic strength (LTP versus LTD) is believed to be determined by the amount of postsynaptic activity (as indexed by Ca^{2+} influx) that occurs during induction: a small amount of postsynaptic Ca^{2+} influx results in LTD, while a larger amount results in LTP (Artola et al., 1990; Mulkey and Malenka, 1992; Hansel et al., 1997; but see Neveu and Zucker, 1996). Moreover, the threshold for eliciting LTP versus LTD may be adjusted by the previous activity of the synapse (Bear et al., 1987).

Inhibitory, GABAergic synapses are also capable of expressing LTP and LTD (Kano, 1995; Marty and Llano, 1995), and in some respects these phenomena are similar to those described for excitatory synapses. For example, all require postsynaptic Ca^{2+} influx (Kano et al., 1992; Komatsu and Iwakiri, 1993; Komatsu, 1996; McLean et al., 1996; Morishita and Sastry, 1996). However, many aspects of these phenomena are unclear. It is not known how GABAergic inhibitory postsynaptic potentials (IPSPs) drive the postsynaptic Ca^{2+} transients that might trigger LTP or LTD. Nor is it known whether a relationship exists between the degree of postsynaptic activation (as indexed by the Ca^{2+} transient) and the direction of long-term synaptic change.

We have addressed these questions by examining a brain region that has been strongly implicated in motor learning. The deep cerebellar nuclei (DCN) are at a crossroads where streams of excitatory and inhibitory inputs, representing a variety of sensorimotor information, converge. The DCN receive excitatory inputs from two sources: mossy fibers, which are the axons of a large number of precerebellar nuclei, and climbing fibers, which are the axons of cells of the inferior olive. The DCN are also the principal target of Purkinje neurons, which are inhibitory and are the sole output of the cerebellar cortex.

There are only two locations in the mammalian brain where learning and memory can be understood at the level of circuits: the cerebellum and the amygdala. In the cerebellum, for example, it is possible to assign the conditioned and unconditioned stimuli in an associative eyeblink conditioning protocol to specific pathways (parallel and climbing fibers, respectively). In contrast, the hippocampus, for all of its experimental utility, receives information that is so highly processed that its content cannot be easily characterized (what is the nature of the information conveyed by the perforant path?). Over the last 15–20 years, a series of experiments that have used behavioral tasks (eyeblink conditioning, vestibulo-ocular reflex (VOR) adaptation) together with extracellular recording, lesion, and inactivation have produced a mixed set of results, with some favoring a locus of information storage at the parallel fiber–Purkinje cell synapse of the cerebellar cortex, and with others implicating the synapses received by the DCN (in the case of eyeblink conditioning), or their analogs, the cells of the medial vestibular nucleus (in the case of VOR adaptation; reviewed by du Lac et al., 1995; Kim and Thompson, 1997). More recently, models have been proposed in which information is sequentially stored, first at cortical and then at deep nuclear locations (Raymond et

‡To whom correspondence should be addressed (e-mail: david.linden@qmail.bs.jhu.edu).

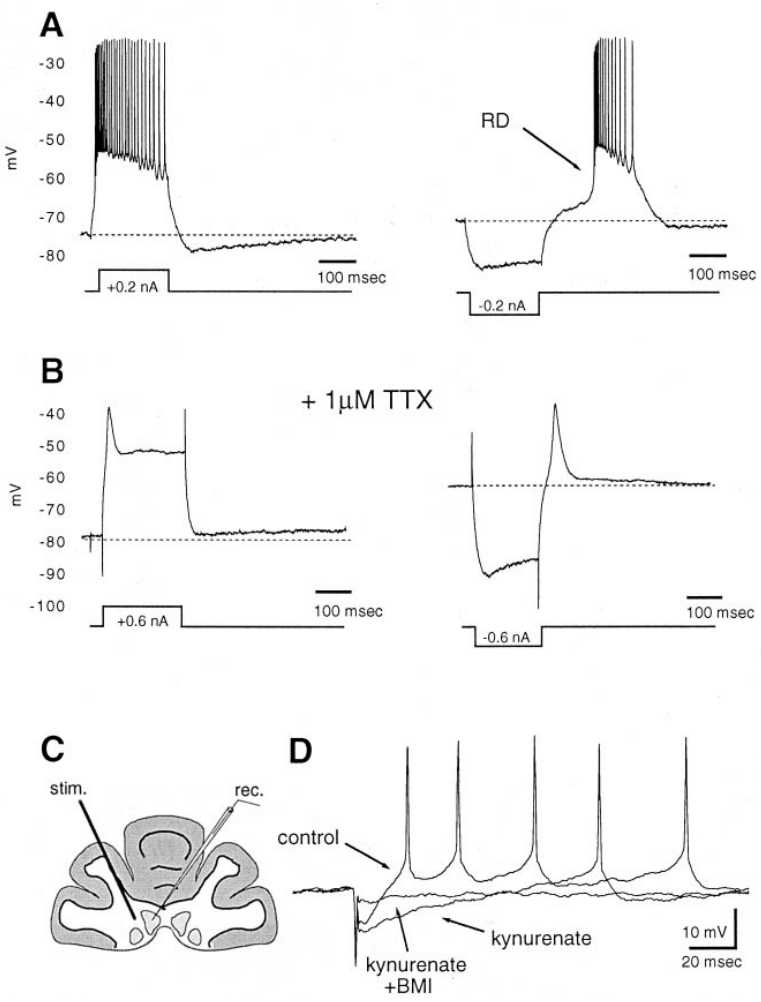

Figure 1. Intrinsic Physiology of DCN Neurons

(A) Sample current-clamp traces from microelectrode recordings in response to a 200 ms depolarizing (left) or hyperpolarizing (right) current pulse in a cell that was held slightly below spike threshold with tonic hyperpolarizing current. Notice the robust RD and associated spike burst that follow the hyperpolarizing pulse.

(B) Sample traces from a different cell in the presence of 1 μM TTX. Although the spike burst is eliminated, the underlying RD remains.

(C) Stimulation and recording configuration in a coronal cerebellar slice.

(D) Synaptic stimulation of white matter evoked a mixed IPSP/EPSP. Its pharmacological components could be revealed with subsequent applications of kynurenate (2 mM) and bicuculline methiodide (BMI, 20 μM).

al., 1996; Mauk, 1997). We have performed intracellular recordings from DCN neurons in slices of rat cerebellum in order to address the questions of (1) whether bidirectional synaptic plasticity exists in the inhibitory synapses to the DCN, supporting the role for this structure in learning, and (2) whether these changes follow general computational principles similar to those that underlie long-term plasticity in excitatory synapses.

Results

Initially, we characterized the responses of DCN neurons to current injection and synaptic activation using microelectrode current-clamp recording. The time-averaged membrane potential of the cells ranged between −75 and −50 mV, with an average of −58 ± 1 mV (n = 33). DCN neurons tonically fire fast action potentials at frequencies that are dependent upon the membrane potential of the cell (Llinás and Mühlethaler, 1988) and can in some cases sustain firing frequencies of ≥100 Hz when depolarized with positive current pulses (Figure 1A). A prominent rebound depolarization (RD) can be elicited upon release from a hyperpolarizing current pulse (Jahnsen, 1986; Llinás and Mühlethaler, 1988; Muri and Knöpfel, 1994; Mouginot and Gähwiler, 1995). Typically, this RD will evoke a burst of fast action potentials (Figure 1A). The RD depends on the membrane potential of the cell during the current pulse and is more reliably evoked when the cell is held in current-clamp mode at potentials more positive than −60 mV and when the hyperpolarizing pulse is sufficiently large. The underlying RD remains when Na^+ action potentials are blocked with tetrodotoxin (TTX) (Figure 1B). Taken together, these results suggest that the RD is evoked when the hyperpolarizing step deinactivates low-threshold, voltage-activated Ca^{2+} channels (T-type), which are then available to open upon return to the holding potential. The time course of the RD may also be modulated by the hyperpolarization-activated cation current, I_h (McCormick and Pape, 1990). Unfortunately, potent and specific antagonists of T-type Ca^{2+} channels are not presently available, and the compounds that are vary considerably in their effects on different neuronal types. In our hands, a wide range of putative T-type Ca^{2+} channel antagonists (ethosuximide, 1 mM; mibefradil, 1 μM; Ni, 100 μM) failed to significantly alter the RD (data not shown).

To evoke synaptic responses in DCN neurons, a stimulating electrode was placed in the white matter immediately adjacent to the DCN (Figure 1C). Stimulation at

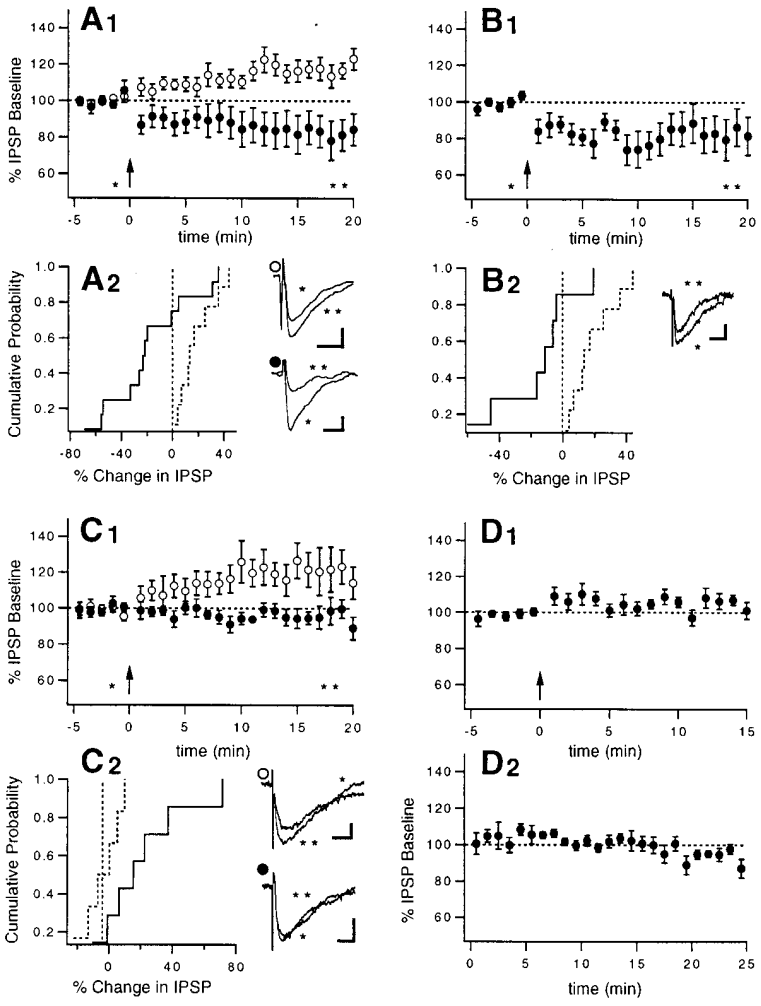

Figure 2. Bidirectional Synaptic Plasticity of IPSPs in the DCN

(A_1) Normalized and averaged time course reflecting changes in IPSP amplitude induced by a burst protocol (applied at arrow; see text). Open circles represent synaptic changes when the burst-protocol is applied while the cell is at resting membrane potential, effectively driving the RD and associated spike burst; closed circles correspond to average changes occurring when the same protocol is applied while the cell is tonically hyperpolarized, thus reducing the amount of postsynaptic spike firing. The inset shows sample traces taken immediately before (*) and 20 min after (**) conditioning stimulation.

(A_2) Cumulative probability distribution of amount of change averaged 15–20 min after conditioning stimulation, applied either while the cell was at rest (dotted line), or while it was tonically hyperpolarized (solid line).

(B_1 and B_2) Averaged time course (B_1) and cumulative probability distribution (B_2) (solid line) of changes induced by burst stimulation in cells intracellularly perfused with voltage-gated Na^+ channel blocker, QX-314. Inset is the same as in (A); the dotted line in (B_2) is the same as in (A_2) and was included for comparison.

(C_1 and C_2) Averaged time course (C_1) and cumulative probability distribution (C_2) of changes induced by postsynaptic application of 200 ms hyperpolarizing pulses, which reliably drive the RD and associated spike burst (open circles, solid line), without synaptic stimulation. Closed circles and dashed line represent the same condition but given while the cell was perfused with QX-314. Inset is the same as in (A).

(D_1) Averaged time course showing suppression of conditioning-induced plasticity by intracellular perfusion of BAPTA (100 mM).

(D_2) Averaged baselines collected for 25 min show that no systematic changes occur without conditioning stimulation. While group data for LTP and LTD conditions is presented here for 20 min after the application of an induction protocol, these changes in synaptic strength were seen to persist for the useful life of the recording, which was 30–35 min in some cases (data not shown). Scale bars, 2 mV, 10 ms (A and C); 1 mV, 10 ms (B).

this site evoked a monosynaptic biphasic sequence of hyperpolarization followed by depolarization. This response is likely to result from simultaneous activation of GABAergic axons of the Purkinje cells (the only inhibitory axons running in the white matter that project to the DCN) and glutamatergic axons of the mossy fiber collaterals, as bath application of an antagonist of ionotropic glutamate receptors (kynurenate, 2 mM) abolished the late depolarizing component. The remaining IPSP was blocked by a $GABA_A$ receptor antagonist (bicuculline, 20 μM; Figure 1D). Although a single IPSP can sometimes evoke a small RD, a brief, high-frequency train of IPSPs (100 Hz, 10 pulses) reliably evokes a large RD (Figure 3A). This provides a frequency-dependent mechanism by which inhibitory inputs can drive postsynaptic excitation.

We tested the hypothesis that the IPSP-driven RD may provide a mechanism by which inhibitory activity may undergo use-dependent plasticity. In order to avoid contamination of the inhibitory synaptic responses by excitatory postsynaptic potentials (EPSPs), all subsequent recordings were performed using 2 mM kynurenate in the external saline. To induce long-term changes in the efficacy of the isolated IPSP, a burst stimulation protocol was used that consisted of ten high-frequency trains (100 Hz, 10 pulses) applied at 2 Hz while the DCN neuron was at its resting membrane potential. This form of stimulation reliably evoked RDs and produced LTP that persisted for at least 20 min, the amplitude of which was 118% ± 5% of baseline (mean ± SEM, measured at t = 15–20 min, n = 9; Figure $2A_1$, open circles). The cumulative probability distribution of the amount of change for individual experiments is shown in Figure $2A_2$ (dotted line). In order to test whether LTP of IPSPs was consistent with the computational rule that large amounts of postsynaptic activation induce LTP, while small amounts induce LTD, we performed two different manipulations that would reduce the RD and therefore limit the postsynaptic activity during the induction protocol. Tonically hyperpolarizing the neuron during burst stimulation reduces the strength of the RD, as assessed by the number of spikes evoked (Figure 3A, bottom). If the same burst protocol that is used to evoke LTP is applied while the cell is tonically hyperpolarized (to −67 ± 2 mV with −400 ± 60 pA), then LTD tends to be elicited (82% ± 9% of baseline, n = 12; Figure $2A_1$,

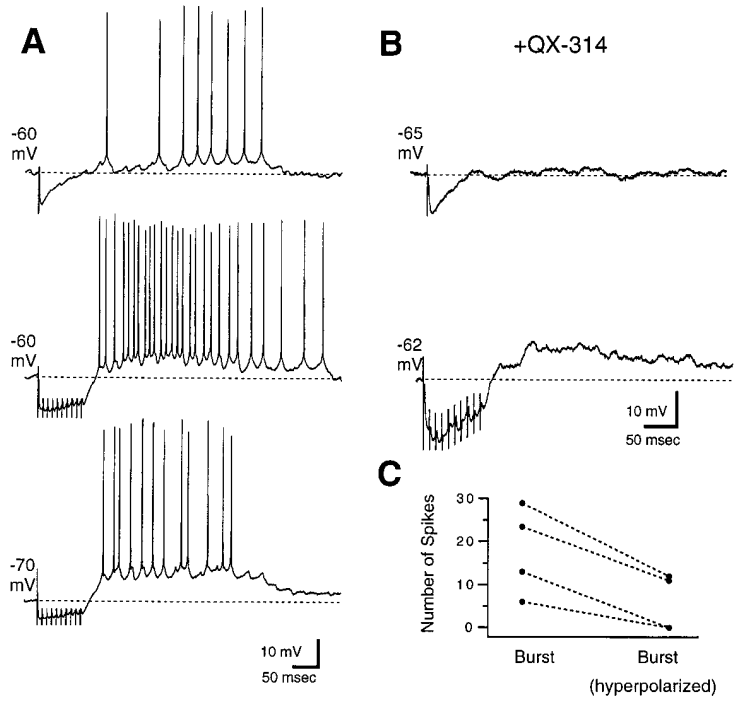

Figure 3. Brief, High Frequency Trains of IPSPs Can Evoke an RD and Associated Spike Firing, which Is Dependent on the Membrane Potential of the Neuron

(A) Sample traces showing an example of spike firing following a single IPSP (top) and following a brief, high-frequency train of IPSPs (100 Hz × 10 pulses, center). The bottom trace illustrates the relative reduction in spiking when the train is applied while the cell is tonically hyperpolarized to −70 mV.

(B) Traces illustrating the absence of spiking following a single IPSP (top) or a train of IPSPs (bottom) in a cell intracellularly perfused with QX-314.

(C) Results from four cells measuring the reduction caused by hyperpolarization in the average number of spikes evoked after a burst of IPSPs. Each point is an average of two RDs.

closed circles). The effect is significantly different from the change caused by the same protocol applied to DCN cells at the resting potential ($p < 0.02$, Mann–Whitney U test), as indicated by the leftward shift in the cumulative probability distribution (Figure $2A_2$, solid line). The second manipulation to limit postsynaptic excitation was intracellular perfusion of the voltage-gated Na^+ channel blocker QX-314. By eliminating Na^+ spikes, QX-314 attenuated the net excitation caused by the burst-evoked RD without eliminating it altogether (Figure 3B) and thereby converted the LTP induction protocol to one that elicits LTD (82% ± 10% of baseline, n = 7; Figure 2B). The effect of the QX-314 on the synaptic gain change induced after burst stimulation is also significant when compared to that induced without QX-314 ($p < 0.01$). QX-314 had no effect on baseline responses over a 25 min period (102% ± 2%, n = 4; data not shown). While these results suggest that the IPSP-driven RD is necessary for induction of LTP/LTD, they do not address the issue of whether activation of the RD alone without synaptic activation is sufficient. To test this, we replaced the synaptic burst protocol with a train of ten 200 ms steps of hyperpolarizing current (−0.5 nA) at 2 Hz, a manipulation that maximally evoked RDs. This resulted in LTP that closely matched the LTP elicited by the synaptic burst stimulation (120% ± 10%, n = 7; Figure $2C_1$, open circles). Hyperpolarizing pulses delivered to QX-314-loaded cells failed to produce any significant change in synaptic strength (96% ± 5%, n = 6; Figure $2C_1$, closed circles), indicating that Na^+ spiking is necessary for this process.

NMDA receptor–dependent LTP and LTD of excitatory synapses (Mulkey and Malenka, 1992; Lynch et al., 1983), as well as LTP and LTD of GABAergic inhibitory synapses (Kano et al., 1992; Komatsu and Iwakiri, 1993; McLean et al., 1996), are dependent upon postsynaptic Ca^{2+} flux. To determine whether this is also true for the present form of LTP and LTD, DCN cells were loaded with the Ca^{2+} chelator BAPTA. The time-averaged resting membrane potential in BAPTA-loaded cells was lower than normal (−67 ± 2 mV; n = 7); however, no noticeable difference in the IPSPs or their ability to drive the RD was observed. No significant change in synaptic efficacy (105% ± 3% of baseline, n = 7; Figure $2D_1$) was induced by the synaptic burst protocol in this condition, indicating that postsynaptic Ca^{2+} entry is necessary for plasticity to occur. As a further control, Figure $2D_2$ shows that baseline responses do not systematically drift over time (n = 7).

The RD can vary considerably among different DCN neurons. However, for any given cell, tonic hyperpolarization always reduces the strength of the RD relative to that evoked while the cell is at rest. Figure 3A illustrates an example of an IPSP train–evoked RD at two different holding potentials. Note that the strength of the RD, as assessed by the number of Na^+ spikes evoked, is reduced when the neuron is held at −70 mV relative to −60 mV. This is a general feature of DCN cells as revealed by analysis of a small population (Figure 3C; n = 4). Cell-to-cell variability in the RD may account for some of the variability in the amount of LTP or LTD elicited by different stimulation conditions. Tetanic bursts of IPSPs strongly activate the postsynaptic cell via the RD, eliciting LTP. However, in the conditions that limit the postsynaptic activity (tonic hyperpolarization, QX-314 perfusion), the same protocol tends to elicit LTD instead. In these conditions, LTD induction was less consistent, sometimes yielding LTP (3/19 cases, for both conditions combined). This suggests that there is either variability in the ability of IPSPs to evoke an RD or perhaps different modification thresholds across the population of neurons. Nevertheless, if all of the experiments across the

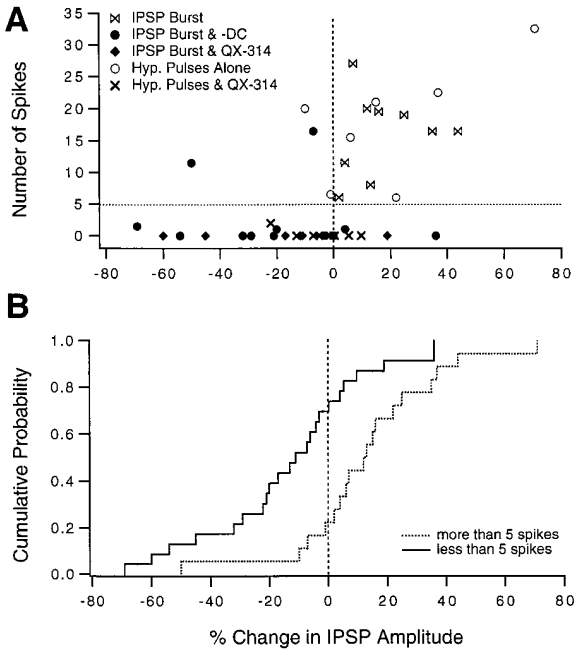

Figure 4. RD-Driven Spike Firing Correlates with the Polarity of Long-Term Synaptic Change

(A) The amount of change caused by conditioning stimulation (averaged 15–20 min postconditioning) is plotted as a function of the average number of RD-driven spikes evoked during the conditioning, across all of the conditions described in Figure 2.

(B) The same data as in (A), replotted as a cumulative probability histogram. The dotted line represents experiments that showed an average of more than five RD-driven spikes; the solid line represents experiments with five or less RD-driven spikes.

different conditions are taken together, a clear pattern emerges. Figure 4A shows the change in IPSP amplitude produced by burst or hyperpolarizing step stimulation as a function of the average number of RD-driven spikes during the initial part of the induction protocol. This reveals a relationship between the number of spikes evoked and the polarity of the synaptic change. Whereas LTP tends to be induced under conditions in which robust RD-driven spiking is present (113% $\pm$ 6%, n = 18), LTD tends to be induced when the RD is elicited (87% $\pm$ 6%, n = 23) but drives little or no spiking ($\leq$5 spikes). The same data is replotted as a cumulative probability histogram (Figure 4B), where each group is plotted as a separate curve, highlighting the difference between the two. The difference between these two groups is statistically significant (p = 0.0015). However, for those cells that showed robust RD-driven spiking, there was only a weak correlation between the number of spikes evoked and the amount of change in synaptic strength (r = +0.452, p = 0.06, n = 18, Pearson r test).

The relationship between RD-evoked spike firing and LTP/LTD, combined with the observation that postsynaptic Ca^{2+} is required for synaptic plasticity to occur, prompted us to measure intracellular Ca^{2+} transients while systematically varying RD-driven spiking. Figure 5A shows the response of a representative Fluo-3-loaded cell to 200 ms hyperpolarizing current pulses, followed by a return to either the holding level or slightly depolarized levels for an additional 300 ms. Upon return to the holding level, a subthreshold depolarization is produced (Figure $5A_1$). When the membrane potential following the hyperpolarizing step is systematically increased, an increasingly strong train of action potentials is evoked. The corresponding fluorescence changes observed at the soma and in a proximal dendrite (Figure 5C) are also shown (Figures $5B_1$ and $5B_2$). With a subthreshold RD, a small, weak Ca^{2+} influx was observed (in 2/5 Fluo-3-loaded cells); however, when the cell discharged action potentials, a much larger intracellular Ca^{2+} transient was detected whose amplitude was proportional to the degree of spiking. In every case (5/5 cells loaded with Fluo-3 and 2/2 cells loaded with Calcium Green-1, the latter of which are not shown), the Ca^{2+} levels increased with increasing discharge rates, and only small or undetectable signals were associated with the subthreshold RD (Figure 5D). These results confirm the notion that the RD alone is not providing a large Ca^{2+} influx, whereas higher intracellular Ca^{2+} concentrations are provided by the opening of Ca^{2+} channels during action potentials. Furthermore, they suggest that the amplitude of RD-evoked Ca^{2+} transients is a critical factor in determining whether LTP or LTD of IPSPs is induced.

Discussion

The main finding of this study is that Purkinje cell–DCN inhibitory synapses can express long-term, bidirectional synaptic plasticity. LTP is induced by high-frequency trains of IPSPs, which reliably evoke an RD, an associated spike burst, and a large Ca^{2+} transient. Conditions that limit RD-evoked spiking and the associated Ca^{2+} transients will result in LTD. RD-driven spiking appears to be both necessary and sufficient to induce LTP. Thus, a major computational feature of excitatory synapses, that moderate postsynaptic activation evokes LTD while strong postsynaptic activation evokes LTP, is also present in this inhibitory synapse.

The amplitudes of LTP and LTD induced herein are smaller than those typically observed in excitatory synapses. However, because inhibitory synapses have a much more powerful integrative effect on cell firing than excitatory synapses, relatively small changes in the strength of inhibitory synapses will have large effects on the integrated output of the postsynaptic cell. The power of inhibitory synapses derives from their location, interposed between excitatory synapses and the spike initiation zone and thereby allowing for the negation of a large number of excitatory synapses by shunting. This has been shown by many investigators, using recording in different brain regions, as well as in modeling studies (Koch et al., 1983). For example, in paired recordings, single IPSPs initiated by perisomatic inhibitory cells could suppress the repetitive discharge of Na^{+} spikes in a hippocampal pyramidal cell (Miles et al., 1996). Thus, it is likely that the LTP and LTD seen herein will have a much larger effect on the output of the postsynaptic cell than would typical LTP (150% of baseline) of an excitatory hippocampal synapse.

It is interesting to consider the degree to which the

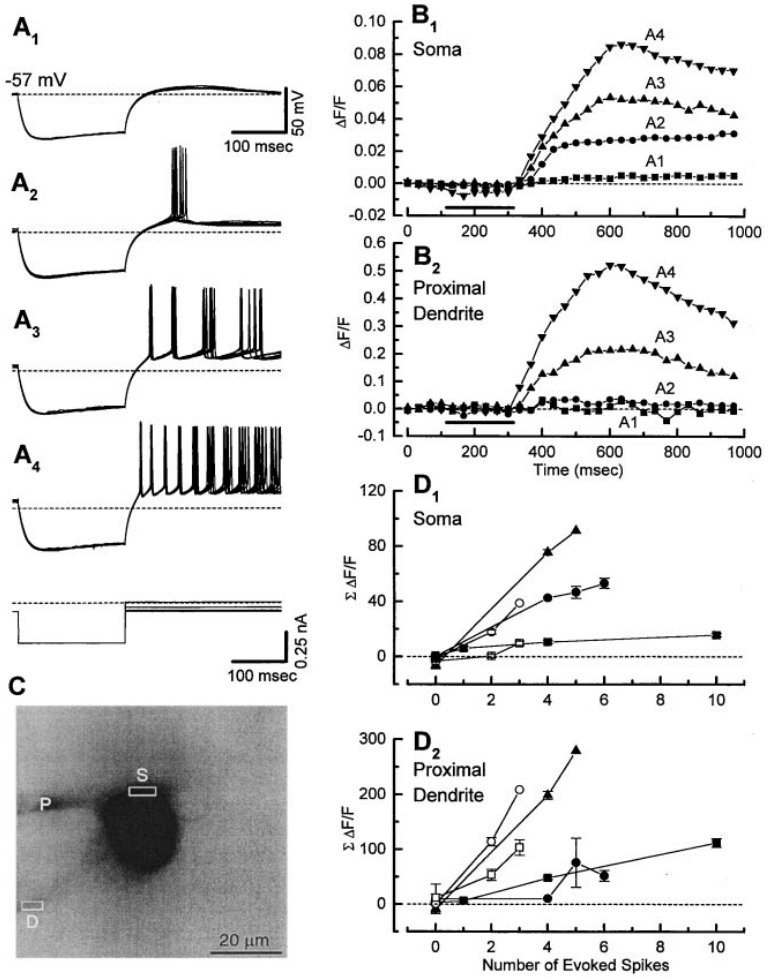

Figure 5. Intracellular Ca^{2+} Transients Are Evoked by RD-Driven Spike Firing

(A) Superimposed recordings of membrane potential during 5–8 trials, as a function of an increasing posthyperpolarizing current injection, as shown in the current traces below A_4.

(B_1) Fluorescence transients recorded from the soma of the cell (each trace is the average of 5–8 trials). Bar below traces shows the duration and timing of the hyperpolarizing current pulses in (A). Small transients are seen with subthreshold RDs (closed squares, data taken simultaneously with traces in [A_1]). Larger transients are seen with more action potentials (closed circles, triangles, and inverted triangles correspond to data taken simultaneously with traces in [A_2], [A_3], and [A_4], respectively).

(B_2) Data taken from the proximal dendrite, ~30 μm from the soma.

(C) Negative fluorescence image of the cell whose data are shown in (A) and (B). "P" is the pipette, "S" indicates the region analyzed for the somatic Ca^{2+}, and "D" indicates the region analyzed for the proximal dendrite.

(D) Summary of fractional changes, integrated for 330 ms ($\Sigma\Delta F/F$) following the offset of the hyperpolarizing pulse, for five Fluo-3-filled cells. Although the slope of the function relating the fractional Ca^{2+} signal to the number of action potentials varied between cells, in general increasing numbers of action potentials produced increasing intracellular Ca^{2+} loads. Matching symbols in (D_1) and (D_2) correspond to the same cell; error bars are standard error of the mean.

cellular mechanisms for use-dependent bidirectional modification differ at excitatory versus inhibitory synapses. One common element is that both excitatory (Lynch et al., 1983; Mulkey and Malenka, 1992) and inhibitory (Kano et al., 1992; Komatsu and Iwakiri, 1993; McLean et al., 1996; Morishita and Sastry, 1996) synapses require postsynaptic Ca^{2+} entry in order to induce synaptic plasticity. In our experiments, suppression of plasticity by postsynaptic BAPTA indicates that Ca^{2+} is also required. In excitatory synapses, postsynaptic Ca^{2+} enters via the activation of NMDA receptors (Collingridge et al., 1983) and/or voltage-gated Ca^{2+} channels (Grover and Teyler, 1990). In the present report, ionotropic glutamate receptors were routinely blocked, and the remaining IPSPs drove postsynaptic excitation by evoking an RD. The RD in DCN cells is thought to be triggered by a low-threshold Ca^{2+} spike that results from the opening of T-type Ca^{2+} channels (Jahnsen, 1986; Llinás and Mühlethaler, 1988; Muri and Knöpfel, 1994; Mouginot and Gähwiler, 1995) and that has been shown to transiently increase intracellular Ca^{2+} concentrations (Muri and Knöpfel, 1994). Indeed, it has been shown in hippocampal pyramidal cells and neocortical neurons that a significant fraction of Ca^{2+} entry during subthreshold excitatory synaptic stimulation is mediated by low-threshold Ca^{2+} channels (Miyakawa et al., 1992; Markram and Sakmann, 1994; Magee et al., 1995). However, this is not likely to be the only source of Ca^{2+} influx during the RD, as the RD can evoke Na^+ spiking. While Na^+ spiking does not produce a direct Ca^{2+} influx, Na^+ action potentials, which are triggered in the initial segment of the axon, can backpropagate via active conductances into the dendritic arbor, causing large transient increases in intracellular Ca^{2+} mediated by opening of high-threshold voltage-gated Ca^{2+} channels (Stuart et al., 1997). Our experiments, as well as previous work (Muri and Knöpfel, 1994), suggest that in the cells of the DCN, a majority of depolarization-evoked Ca^{2+} entry is associated with Na^+ spikes. Furthermore, it has been shown that LTP of EPSPs in pyramidal neurons can be elicited by pairing postsynaptic spikes with low-frequency synaptic stimulation (Magee and Johnston, 1997; Markram et al., 1997). Backpropagating spikes can therefore act as a "coincidence" signal that can sum pre- and postsynaptic activation through a contribution to the dendritic Ca^{2+} transient.

It is worthwhile to note that in DCN cells, the duration of the Ca^{2+} transients considerably outlasted the duration of spiking (Figure 5), raising the possibility that the Ca^{2+} transient did not solely reflect Ca^{2+} channel opening during spiking. However, it is not unusual for Ca^{2+} transients evoked by spike bursts to outlast these bursts by 500–2000 ms in a number of neurons, including DCN

cells (Muri and Knöpfel, 1994) and hippocampal pyramidal cells (Jaffe et al., 1992). In fact, Markram et al. (1995) showed Ca^{2+} transients evoked by a single spike in neocortical pyramidal cells that required ~1200 ms to decay to baseline. In addition, it is possible that the Ca^{2+} signals we record could have components that are driven by voltage-sensitive Ca^{2+} channels activated by plateau potentials that may outlast spiking, or by Ca^{2+} mobilization from internal stores. Furthermore, there exists yet another mechanism by which high-frequency bursts of IPSPs may drive postsynaptic Ca^{2+}. $GABA_A$ receptor channels usually carry a Cl^- influx but are also permeable to HCO_3^-. Prolonged high-frequency activation of $GABA_A$ receptors can lead to a transient depletion of the Cl^- gradient, resulting in an efflux of HCO_3^-, and a consequent depolarizing response (Kaila et al., 1993; Staley et al., 1995). This scenario is unlikely in our preparation due to the fact that the RD can be induced by hyperpolarizing pulses alone. In addition, while there can be some accommodation of the IPSPs during brief trains, we do not observe a reversal of the IPSPs (see Figure 3).

We propose the following model to describe use-dependent plasticity in the Purkinje cell–DCN synapse. First, high-frequency trains of IPSPs will cause low-threshold Ca^{2+} channels to open upon release from hyperpolarization, leading to a small Ca^{2+} influx in the dendritic arbor. This would be sufficient to induce LTD. Second, if this depolarization is sufficiently large, it will depolarize the cell soma past the threshold for Na^+ spiking. Third, the Na^+ spikes will then backpropagate into the dendritic arbor, where they will induce the activation of high-threshold Ca^{2+} channels, further increasing the intracellular Ca^{2+} transient and reaching the threshold for LTP induction. Our data support this model, because conditioning that strongly evokes the RD and Na^+ spiking (IPSP trains at resting membrane potential, hyperpolaring pulses alone) induces LTP as well as large intracellular Ca^{2+} transients, while conditioning given under limiting conditions (tonic hyperpolarization, QX-314) reduces Na^+ spiking but does not eliminate the underlying RD and thus tends to induce LTD. Due to a lack of a specific and potent antagonist, it is not presently possible to test directly the role of low-threshold Ca^{2+} channels. It is worthwhile to note that the key computational feature of this model, that RD-evoked spiking correlates with both the amplitude of the postsynaptic Ca^{2+} transient and the induction of LTP/LTD, would remain intact even if additional sources of Ca^{2+} (see above) were found to contribute to the transient.

In our hands, hyperpolarizing pulses given in the presence of QX-314 (which completely abolished spiking) resulted in no alteration of synaptic strength (Figure 2C). We show in Figure 5B that a hyperpolarizing pulse-evoked rebound depolarization that is subthreshold for spike generation produces little or no Ca^{2+} transient. Thus, it is consistent with our model that no change in synaptic strength is evoked. This finding contrasts with the observation that synaptic stimulation in the presence of QX-314 resulted in LTD (Figure 2B), suggesting that the RD generated by synaptic inputs (which are all over the cell) is probably qualitatively different than that induced by an electrode (a point source) at the soma. Perhaps a protocol could be developed in which hyperpolarizing pulses would produce minimal spiking, and a small dendritic Ca^{2+} transient, and thereby induce LTD. However, it should be emphasized that this could be difficult due to the variability in dendritic Ca^{2+} transients produced by somatic hyperpolarization (Figure 5D).

Our data suggest a novel solution for a long-standing problem in cellular synaptic plasticity: how do inhibitory synapses produce postsynaptic Ca^{2+} signals that are required for use-dependent plasticity when they do not directly gate a Ca^{2+} conductance? A number of studies in various brain regions have found that LTP or LTD of inhibitory synapses can be blocked by postsynaptic application of a Ca^{2+} chelator. However, the proposed source(s) of this Ca^{2+} transient have varied widely across preparations. One explanation has been that the Ca^{2+} transient is not directly triggered by the IPSP. For example, in "rebound potentiation" in the cerebellar interneuron–Purkinje cell synapse, the Ca^{2+} transient is driven by coincident activation of excitatory climbing fibers, resulting in the subsequent activation of voltage-gated Ca^{2+} channels (Kano et al., 1992). Likewise, it has been shown that LTD of IPSPs in neonatal hippocampus (McLean et al., 1996) and LTD of the Purkinje cell–DCN IPSPs in 5- to 9-day-old rat cerebellum (Morishita and Sastry, 1996) require coincident activation of NMDA receptors. A second explanation, which comes from studies of developing visual cortex, is that activation of postsynaptic $GABA_B$ receptors potentiates phosphatidylinositol (PI) turnover and subsequent Ca^{2+} mobilization driven by adrenergic innervation, thus inducing LTP of inhibition (Komatsu, 1996). Finally, it has been shown that in early development of the hippocampus (≤P5), depolarizing IPSPs can directly activate voltage-sensitive Ca^{2+} channels, thereby contributing to LTP of these synapses (McLean et al., 1996). Because the experiments in our manuscript were conducted with excitatory synapses blocked, it became possible to study the capacity for inhibitory synapses to undergo use-dependent modification in isolation. Our finding that the IPSP-driven rebound depolarization and subsequent spiking is the key determinant of LTP and LTD induction in this synapse is computationally significant, in that it describes a mechanism for inhibitory synapses to undergo LTP and LTD in a manner that does not require interaction with noninhibitory synapses and that can function throughout the life span of the animal (in mature synapses with hyperpolarizing IPSPs).

There are a number of avenues for future experimentation that are opened by the present observations. At a cellular level, it will be interesting to determine the biochemical mechanisms that couple RD-driven Ca^{2+} influx to LTP and LTD of IPSPs. In glutamatergic synapses, low and high postsynaptic Ca^{2+} signals have been suggested to differentially activate protein phosphatase 1 and Ca^{2+}/calmodulin-dependent protein kinase II, respectively (Lisman, 1989; Mulkey et al., 1993, 1994), resulting in dephosphorylation and phosphorylation of postsynaptic AMPA receptors. Similar mechanisms may be operative in inhibitory synapses. It has been shown that blockade of protein phosphatase activity can attenuate 10 Hz–induced LTD in Purkinje cell–DCN synapses (Morishita and Sastry, 1996). Inhibition

of Ca^{2+}/calmodulin-dependent protein kinase II has also been shown to block LTP of GABAergic interneuron–Purkinje cell synapses in the cerebellar cortex (Kano et al., 1992, 1996). However, this may not be a common mechanism for all GABAergic synapses, as the α isoform of this enzyme is not found at GABAergic synapses in the neocortex, thalamus, and hippocampus (Liu and Jones, 1996, 1997).

At a phenomenological level, it will be interesting to determine if the present forms of LTP and LTD are saturable, reversible, and input specific. One prediction of our model would be that LTD would tend to have a greater degree of input specificity than LTP, due to the broad invasion of the dendritic arbor by backpropagating spikes in the latter case. Another prediction is that cross talk may occur between glutamatergic and GABAergic inputs to the cells of the DCN. This could provide a mechanism by which mossy fiber–driven Ca^{2+} signals could produce LTP/LTD of GABAergic synapses, or vice versa, and is consistent with previous observations that NMDA receptor activation can trigger LTD of IPSPs in the DCN (Morishita and Sastry, 1996). An interesting interpretation of these data is that LTP and LTD of IPSPs may serve as a synaptic "homeostatic" mechanism to regulate the overall excitability and dynamic range of the DCN cell. Thus, large amounts of postsynaptic spiking will potentiate IPSPs, making the cell less likely to fire more action potentials, whereas LTD tends to be induced when the postsynaptic activity is limited, increasing the probability of postsynaptic spiking. The details of these phenomena will be of great importance in building models of cerebellar motor learning that incorporate synaptic information storage at both cortical and DCN loci (Raymond et al., 1996; Mauk, 1997).

Experimental Procedures

Slice Preparation and Electrophysiology

Microelectrode recordings were made from the deep nuclei in 400 μm thick coronal slices from 11- to 15-day-old rat cerebellum. Slices were cut using a Vibratome and were incubated in ice-cold standard artificial cerebrospinal fluid (ACSF) containing (in mM): NaCl (126), KCl (5), $CaCl_2$ (2), $MgSO_4$ (2), $NaHCO_3$ (26), NaH_2PO_4 (1.25), and D-glucose (20) and continuously bubbled with 95% O_2, 5% CO_2. They were then incubated for at least 1 hr at room temperature in a homemade interface chamber, following which recordings were performed in a Haas-style interface chamber at 33°C that was perfused with ACSF containing 2 mM kynurenate to block ionotropic glutamate receptors. Borosilicate glass microelectrodes (80–150 MΩ) were filled with 3 M KAc. Concentric bipolar stimulating electrodes were placed in the white matter immediately adjacent to the nuclei. Recordings were made from either the medial or lateral group of the DCN, and no differences were observed between the two nuclei. Stimulation intensities were used that evoked IPSPs between 50%–70% of maximum, and baseline traces were acquired every 30 s. For the LTP and LTD experiments, the input resistance of the cell was monitored after every trace, and experiments were discarded if the input resistance varied by >20% or if this change was >50% of the change in IPSP amplitude. However, no significant overall changes in the input resistance were observed in any of the conditions described. During acquisition of baseline, the cells were hyperpolarized in order to prevent spontaneous Na^+ spikes but were always manually clamped at voltages above the reversal potential of the IPSP. In some experiments (Figure $2D_1$), 100 mM BAPTA was included in the internal solution and was allowed to perfuse into the cell for at least 20 min before burst stimulation was applied. Where indicated, 100 mM QX-314 was included in the internal solution, and recording was begun after the Na^+ action potentials ceased, typically 5–10 min after impalement. In Figure 2, samples were collected every 30 s and every two samples were averaged. IPSP amplitudes were then normalized to baseline ($t = -5$ to 0 min), and are expressed as the mean $\pm$ SEM. When different conditions are compared statistically, p is derived using the Mann–Whitney U test.

Ca^{2+} Imaging

Imaging of Ca^{2+} transients was performed with 250 μm thick slices cut and maintained as described above. The slices were placed in a heated submersion chamber on a fixed-stage microscope and imaged with a 40× 0.65 NA water immersion objective. Whole-cell tight-seal recordings were made under direct vision using pipettes made from KG33 glass, filled with (in mM): K-gluconate (110), KCl (20), NaCl (4), Mg-ATP (4), phosphocreatine (10), GTP (0.3), HEPES (10), and Fluo-3 K salt (0.2) or Calcium Green-1 K salt (0.2) (pH 7.2 with KOH). Electrical recordings were made with a List EPC−7 in current-clamp mode. Fluo-3 or Calcium Green-1 was excited by light from a mercury arc lamp (HBO100) passed through a 450–490 bandpass filter and an FT510 dichroic mirror. The emitted light from the fluorophores was passed through a 520 longpass filter and was collected by a Cohu 4982 CCD camera at 10 bits through a DD2000 frame grabber board (Axon Instruments), controlled by Axon Imaging Workbench (AIW, version 2.0192). To ensure synchrony of the physiological and optical data, the falling edge of the trigger output of AIW was used to reset the camera vertical sync signal and to trigger electrophysiological acquisition. Data were collected at video rate (33 ms/frame) in small regions and analyzed offline. Calculations of fractional changes in fluorescence over selected regions were computed by subtracting the background fluorescence in a region near the cell with no visible processes, and by normalizing the data by the resting fluorescence determined from the average of the first two (unstimulated) frames. Occasional image sequences revealed excessive delays by AIW or artifacts from arc wandering (visible in the background light levels) and were not included in the analysis.

Acknowledgments

Thanks to K. Takahashi, C. Hansel, H.-K. Lee, and A. Kirkwood for helpful comments on an earlier version of the manuscript. This work was supported by the Develbiss Fund (D. J. L.), an HHMI Predoctoral Fellowship (C. D. A.), and NIDCD grant R01 DC00425 (P. B. M.).

Received June 1, 1998; revised July 27, 1998.

References

Artola, A., Bröcher, S., and Singer, W. (1990). Different voltage-dependent thresholds for inducing long-term depression and long-term potentiation in slices of rat visual cortex. Nature *347*, 69–72.

Bear, M.F., and Malenka, R.C. (1994). Synaptic plasticity: LTP and LTD. Curr. Opin. Neurobiol. *4*, 389–399.

Bear, M.F., Cooper, L.N., and Ebner, F.F. (1987). A physiological basis for a theory of synapse modification. Science *237*, 42–48.

Collingridge, G.L., Kehl, S.J., and McLennan, H. (1983). Excitatory amino acids in synaptic transmission in the Schaffer collateral–commissural pathway of the rat hippocampus. J. Physiol. (Lond.) *334*, 33–46.

du Lac, S., Raymond, J.L., Sejnowski, T.J., and Lisberger, S.G. (1995). Learning and memory in the vestibulo-ocular reflex. Annu. Rev. Neurosci *18*, 409–441.

Grover, L.M., and Teyler, T.J. (1990). Two components of long-term potentiation induced by different patterns of afferent activation. Nature *347*, 477–479.

Hansel, C., Artola, A., and Singer, W. (1997). Relation between dendritic Ca^{2+} levels and the polarity of synaptic long-term modifications in rat visual cortex neurons. Eur. J. Neurosci. *9*, 2309–2322.

Jaffe, D.B., Johnston, D., Lasser-Ross, N., Lisman, J.E., Miyakawa, H., and Ross, W.N. (1992). The spread of Na^+ spikes determines

the pattern of dendritic Ca^{2+} entry into hippocampal neurons. Nature *357*, 244–246.

Jahnsen, H. (1986). Electrophysiological characteristics of neurones in the guinea-pig deep cerebellar nuclei in vitro. J. Physiol. (Lond.) *372*, 129–147.

Kaila, K., Voipio, J., Paalasmaa, P., Pasternack, M., and Deisz, R.A. (1993). The role of bicarbonate in $GABA_A$ receptor–mediated IPSPs of rat neocortical neurones. J. Physiol. (Lond.) *464*, 273–289.

Kano, M. (1995). Plasticity of inhibitory synapses in the brain: a possible memory mechanism that has been overlooked. Neurosci. Res. *21*, 177–182.

Kano, M., Rexhausen, U., Dreessen, J., and Konnerth, A. (1992). Synaptic excitation produces a long-lasting rebound potentiation of inhibitory synaptic signals in cerebellar Purkinje cells. Nature *356*, 601–604.

Kano, M., Kano, M., Fukunaga, K., and Konnerth, A. (1996). Ca^{2+}-induced rebound potentiation of gamma-aminobutyric acid–mediated currents requires activation of Ca^{2+}/calmodulin-dependent kinase II. Proc. Natl. Acad. Sci. USA *93*, 13351–13356.

Kim, J.J., and Thompson, R.F. (1997). Cerebellar circuits and synaptic mechanisms involved in classical eyeblink conditioning. Trends Neurosci. *20*, 177–181.

Koch, C., Poggio, T., and Torre, V. (1983). Nonlinear interactions in a dendritic tree: localization, timing and role in information processing. Proc. Natl. Acad. Sci. USA *80*, 2799–2802.

Komatsu, Y. (1996). $GABA_B$ receptors, monoamine receptors, and postsynaptic inositol trisphosphate–induced Ca^{2+} release are involved in the induction of long-term potentiation at visual cortical inhibitory synapses. J. Neurosci. *16*, 6342–6352.

Komatsu, Y., and Iwakiri, M. (1993). Long-term modification of inhibitory synaptic transmission in developing visual cortex. Neuroreport *4*, 907–910.

Linden, D.J., and Connor, J.A. (1995). Long-term synaptic depression. Annu. Rev. Neurosci. *18*, 319–357.

Lisman, J. (1989). A mechanism for the Hebb and the anti-Hebb processes underlying learning and memory. Proc. Natl. Acad. Sci. USA *86*, 9574–9578.

Lisman, J. (1994). The CaM kinase II hypothesis for the storage of synaptic memory. Trends Neurosci. *17*, 406–412.

Liu, X.-B., and Jones, E.G. (1996). Localization of alpha type II calcium calmodulin–dependent protein kinase at glutamatergic but not gamma-aminobutyric acid (GABAergic) synapses in thalamus and cerebral cortex. Proc. Natl. Acad. Sci. USA *93*, 7332–7336.

Liu, X.-B., and Jones, E.G. (1997). Localization of alpha-type II calcium/calmodulin-dependent protein kinase specifically at glutamatergic synapses in rat hippocampus. Neuroreport *8*, 1475–1479.

Llinás, R., and Mühlethaler, M. (1988). Electrophysiology of guinea-pig cerebellar nuclear cells in the in vitro brain stem–cerebellar preparation. J. Physiol. (Lond.) *404*, 241–258.

Lynch, G., Larson, J., Kelso, S., Barrionuevo, G., and Schottler, F. (1983). Intracellular injections of EGTA block induction of hippocampal long-term potentiation. Nature *305*, 719–721.

Magee, J.C., and Johnston, D. (1997). A synaptically controlled, associative signal for Hebbian plasticity in hippocampal neurons. Science *275*, 209–213.

Magee, J.C., Christofi, G., Miyakawa, H., Christie, B., Lasser-Ross, N., and Johnston, D. (1995). Subthreshold synaptic activation of voltage-gated Ca^{2+} channels mediates a localized Ca^{2+} influx into the dendrites of hippocampal pyramidal neurons. J. Neurophysiol. *74*, 1335–1342.

Markram, H., and Sakmann, B. (1994). Calcium transients in dendrites of neocortical neurons evoked by single subthreshold excitatory postsynaptic potentials via low-voltage-activated calcium channels. Proc. Natl. Acad. Sci. USA *91*, 5207–5211.

Markram, H., Helm, P.J., and Sakmann, B. (1995). Dendritic calcium transients evoked by single back-propagating action potentials in rat neocortical pyramidal neurons. J. Physiol. (Lond.) *485*, 1–20.

Markram, H., Lübke, J., Frotscher, M., and Sakmann, B. (1997). Regulation of synaptic efficacy by coincidence of postsynaptic APs and EPSPs. Science *275*, 213–215.

Marty, A., and Llano, I. (1995). Modulation of inhibitory synapses in the mammalian brain. Curr. Opin. Neurobiol. *5*, 335–341.

Mauk, M.D. (1997). Roles of cerebellar cortex and nuclei in motor learning: contradictions or clues? Neuron *18*, 343–346.

McCormick, D.A., and Pape, H.-C. (1990). Properties of a hyperpolarization-activated cation current and its role in rhythmic oscillation in thalamic relay neurones. J. Physiol. (Lond.) *431*, 291–318.

McLean, H.A., Caillard, O., Ben-Ari, Y., and Gaiarsa, J.L. (1996). Bidirectional plasticity expressed by GABAergic synapses in the neonatal rat hippocampus. J. Physiol. (Lond.) *496*, 471–477.

Miles, R., Tóth, K., Gulyás, A.I., Hájos, N., and Freund, T.F. (1996). Differences between somatic and dendritic inhibition in the hippocampus. Neuron *16*, 815–823.

Miyakawa, H., Ross, W.N., Jaffe, D., Callaway, J.C., Lasser-Ross, N., Lisman, J.E., and Johnston, D. (1992). Synaptically activated increases in Ca^{2+} concentration in hippocampal CA1 pyramidal cells are primarily due to voltage-gated Ca^{2+} channels. Neuron *9*, 1163–1173.

Morishita, W., and Sastry, B.R. (1996). Postsynaptic mechanisms underlying long-term depression of GABAergic transmission in neurons of the deep cerebellar nuclei. J. Neurophysiol. *76*, 59–68.

Mouginot, D., and Gähwiler, B.H. (1995). Characterization of synaptic connections between cortex and deep nuclei of the rat cerebellum in vitro. Neuroscience *64*, 699–712.

Mulkey, R.M., and Malenka, R.C. (1992). Mechanisms underlying induction of homosynaptic long-term depression in area CA1 of the hippocampus. Neuron *9*, 967–975.

Mulkey, R.M., Herron, C.E., and Malenka, R.C. (1993). An essential role for protein phosphatases in hippocampal long-term depression. Science *261*, 1051–1055.

Mulkey, R.M., Endo, S., Shenolikar, S., and Malenka, R.C. (1994). Involvement of a calcineurin/inhibitor-1 phosphatase cascade in hippocampal long-term depression. Nature *369*, 486–488.

Muri, R., and Knöpfel, T. (1994). Activity induced elevations of intracellular calcium concentration in neurons of the deep cerebellar nuclei. J. Neurophysiol. *71*, 420–428.

Neveu, D., and Zucker, R.S. (1996). Postsynaptic levels of $[Ca^{2+}]_i$ needed to trigger LTD and LTP. Neuron *16*, 619–629.

Raymond, J.L., Lisberger, S.G., and Mauk, M.D. (1996). The cerebellum: a neuronal learning machine? Science *272*, 1126–1131.

Staley, K.J., Soldo, B.L., and Proctor, W.R. (1995). Ionic mechanisms of neuronal excitation by inhibitory $GABA_A$ receptors. Science *269*, 977–981.

Stuart, G., Spruston, N., Sakmann, B., and Häusser, M. (1997). Action potential initiation and backpropagation in neurons of the mammalian CNS. Trends Neurosci. *20*, 125–131.